June 30, 2020

Protein kinase A catalytic-α and catalytic-β proteins have non-redundant functions

Viswanathan Raghuram, Karim Salhadar, Kavee Limbutara,

Euijung Park, Chin-Rang Yang and Mark A. Knepper

Epithelial Systems Biology Laboratory, Systems Biology Center, National Heart, Lung, and Blood Institute, National Institutes of Health, Bethesda, Maryland

‡Correspondence to Mark A. Knepper, National Institutes of Health, Bldg. 10, Room 6N307, 10 CENTER DR, MSC-1603, Bethesda, MD 20892-1603, Phone: (301) 496-3064, Fax: (301) 402-1443, E-mail: knepperm@nhlbi.nih.gov

Running Head: Protein kinase A targets

Keywords: phosphoproteomics, protein kinases, phosphorylation, genome editing, collecting duct, kidney

Supplemental data are deposited at https://hpcwebapps.cit.nih.gov/ESBL/Database/Supplemental_Data_PKA_sKO/.

ABSTRACT

Vasopressin regulates osmotic water transport in the renal collecting duct by PKA-mediated control of the water channel aquaporin-2 (AQP2). Collecting duct principal cells express two seemingly redundant PKA catalytic subunits, PKA catalytic α (PKA-Cα) and PKA catalytic β (PKA-Cβ). To identify the roles of these two protein kinases, we carried out deep phosphoproteomic analysis in cultured mpkCCD cells in which either PKA-Cα or PKA-Cβ was deleted using CRISPR-Cas9-based genome editing. Controls were cells carried through the genome editing procedure, but without deletion of PKA. TMT mass tagging was used for protein mass spectrometric quantification. Of the 4635 phosphopeptides that were quantified 67 were significantly altered in abundance with PKA-Cα deletion, while 21 were significantly altered in abundance with PKA-Cβ deletion. However, only four sites were changed in both. The target proteins identified in PKA-Cα-null cells were largely associated with cell membranes and membrane vesicles, while target proteins in the PKA-Cβ-null cells were largely associated with the actin cytoskeleton and cell junctions. In contrast, in vitro incubation of mpkCCD proteins with recombinant PKA-Cα and PKA-Cβ resulted in virtually identical phosphorylation changes. In addition, analysis of total protein abundances in the in vivo samples showed that PKA-Cα deletion resulted in a near disappearance of AQP2 protein, while PKA-Cβ deletion did not decrease AQP2 abundance. We conclude that PKA-Cα and PKA-Cβ serve substantially different functions in renal collecting duct cells and that differences in phosphorylation targets may be due to differences in protein interactions, e.g. mediated by AKAP, C-KAP or PDZ binding.

INTRODUCTION

Vasopressin's actions in collecting duct principal cells (23) are mediated by a G-protein coupled receptor (GPCR) V2R (Gene symbol: *Avpr2*), which couples to the heterotrimeric G-protein stimulatory α subunit ($G_s\alpha$) with activation of adenylyl cyclase 6 (22). Increased intracellular cyclic AMP levels result in physiological effects in collecting duct principal cells largely through activation of PKA (4, 5, 8, 11, 12, 17, 19-21) . Two of the most important physiological end effects are: 1) membrane trafficking changes that increase the abundance of the water channel protein aquaporin-2 (AQP2) in the plasma membrane (18) and 2) increased transcription of the *Aqp2* gene (7, 14, 24), both of which contribute to vasopressin induced increases in osmotic water transport across the collecting duct epithelium. Protein Kinase A (PKA) is a widely studied protein that has been viewed by most investigators as a single entity, although its catalytic subunits are coded in mammalian genomes by two separate genes, PKA catalytic α (PKA-Cα [Gene symbol: *Prkaca*]) and PKA catalytic β (PKA-Cβ [Gene symbol: *Prkacb*]). At an amino-acid level, the two are 91 percent identical and the catalytic domains are very similar. (Footnote: A third entity PKA catalytic γ, is not widely expressed and will not be considered in this paper.) We have recently succeeded in using CRISPR-Cas9 to create disruptive mutations in both PKA catalytic genes (PKA double KO or PKA dKO) in vasopressin-responsive kidney epithelial cells (mpkCCD cells) (9). We then used phosphoproteomics to identify a large number of novel PKA targets as well as many secondary changes in phosphorylation due to loss of PKA-mediated regulation of other kinases and phosphatases (9). Whether the two PKA catalytic proteins have redundant functions, as is implicitly assumed in many studies involving PKA-mediated regulation, has not been tested. Here, we carry out mass spectrometry-based quantitative proteomics and phosphoproteomics in both PKA catalytic-α and PKA catalytic-β single knockouts in mpkCCD collecting duct cells to address this issue. Thus, the goal of this study is to identify the relative roles of PKA-Cα and PKA-Cβ in the signaling processes triggered by vasopressin.

METHODS

Cell culture

The study utilized immortalized mpkCCD cells in which either *Prkaca* or *Prkacb* gene expression was deleted ("PKA-Cα-null" and "PKA-Cβ-null") by introducing mutations using CRISPR-Cas9 (9). Control cell lines ("PKA-intact") were carried through the CRISPR-Cas9 protocol but did not show deletion of either PKA catalytic gene. We used three independent PKA-Cα-null lines and three independent PKA-intact controls. Similarly, we used three independent PKA-Cβ-null lines and three different independent PKA-intact controls, giving 3 biological replicates for each kinase. Experiments with these lines were performed in duplicate (i.e. 2 technical replicates each) giving 24 samples in total. The overall scheme is summarized in **Figure 1**. Cells were cultured as described previously (13). Briefly, they were initially maintained in complete medium, DMEM/F-12 containing 2% serum and other supplements (5 µg/mL insulin, 50 nM dexamethasone, 1 nM triiodothyronine, 10 ng/mL epidermal growth factor, 60 nM sodium selenite, 5 µg/mL transferrin; all from Sigma). Cells were seeded on permeable membrane supports (Transwell) and grown in complete medium containing 0.1 nM 1-desamino-8-d-arginine-vasopressin (dDAVP, basal side only) for 4 days during which the cells formed confluent monolayers. Then, the medium was changed to simple medium (DMEM/F12 with dexamethasone, sodium selenite, and transferrin and no serum) with 0.1 nM dDAVP and maintained for 3 days at which time the cells were harvested for proteomic analysis. Because dDAVP was present in the culture medium under all conditions, it was not an experimental variable in the present study.

Phosphoproteomics

Sample preparation for total- and phospho-proteomics. Cells were washed three times with ice-cold PBS and lysed with TEAB buffer (ThermoFisher) with SDS (1%) containing protease and phosphatase inhibitors (*Halt*^{TM}, ThermoFisher). The membranes were scraped and samples were homogenized using a QIAshredder (Qiagen). Protein concentrations were measured using the Pierce™

BCA Protein Assay Kit. Protein lysates were reduced with 20 mM dithiothreitol for 1 hour at 25°C, and then alkylated with 40 mM iodoacetamide for 1 hour at 25°C in the dark. The proteins were acetone precipitated prior to digestion with recombinant trypsin (ThermoFisher) (1:50 wt/wt.) overnight at 37°C. The resulting peptides were desalted using hydrophilic-lipophilic-balanced (HLB) extraction cartridges (Oasis) and quantified using Pierce™ Quantitative Colorimetric Peptide Assay. For each replicate, 250 µg of peptide were labeled using TMT11Plex Mass Tag Labeling Kit (Thermo Scientific, Lot number UE283355) following the manufacturer's instructions and they were combined as shown in **Figure 1**. A total of three labeling batches using the same TMT11 Plex Mass Tag kit were run to quantify all 24 samples. Each batch included a common pooled sample containing a mixture of all 24 experimental samples. Samples were combined and, after taking an aliquot for total proteomics, phosphopeptides were sequentially enriched following the Sequential Enrichment from Metal Oxide Affinity Chromatography protocol (SMOAC, Thermo Scientific). We then fractionated the samples (12 fractions) using high pH reverse phase chromatography (Agilent 1200 HPLC System). Samples were then vacuum-dried and stored at -80°C until analysis.

The dried peptides were re-suspended with 0.1% formic acid, 2% acetonitrile in LC-MS grade water (J.T. Baker) before mass spectrometry analysis. Peptides (total and phospho-) were analyzed using a Dionex UltiMate 3000 nano LC system connected to an Orbitrap Fusion Lumos mass spectrometer equipped with an EASY-Spray ion source (Thermo Fisher Scientific). Peptides were introduced into a peptide nanotrap at a flow rate of 5 µL/min. The trapped peptides were fractionated with a reversed-phase EASY-Spray PepMap column (C18, 75 µm × 50 cm) using a linear gradient of 4 to 32% acetonitrile in 0.1% formic acid (120 min at 0.3 µL/min).

Mass spectrometry data processing. Raw mass spectra were searched against the *Mus musculus* UniProtKB(26) reference proteome (Proteome ID: UP000000589, release 2019_06, plus contaminant database) using MaxQuant(2) 1.6.7.0. Quantitative abundance profiling of tandem mass

tag (TMT)-labeled proteins and phosphopeptides were based on Synchronous Precursor Selection-MS3 (SPS-MS3) workflow (16). Lot-specific TMT isotopic impurity correction factors were used as recommended in the TMT product data sheets. Variable modifications included phospho (STY), oxidation (M), and acetyl (Protein-N-terminal). False discovery rate was controlled at 1% (target-decoy). "Trypsin/P" was set as the digestion enzyme with up to 2 missed cleavages allowed. Other parameters were set to the defaults. We used "proteinGroups.txt" output file as the input data for total proteome analyses. Both "Phospho (STY)Sites.txt" and "evidence.txt" output files were used for phosphoproteome analyses. For each TMT batch, corrected reporter ion intensities were first normalized to make the total sum intensities for each channel equal. Then, the average of the common pooled channel from three TMT batches were used to normalize the batch effects.

In vitro phosphorylation experiments. Three independent PKA dKO cell lines (9) were grown on permeable membrane supports as described above. The confluent monolayers were washed three times with ice-cold PBS and lysed with TEAB buffer (ThermoFisher) with SDS (1%) containing protease and phosphatase inhibitors. The membranes were scraped and samples were homogenized using a QIAshredder (Qiagen) and the proteins were precipitated with acetone. The protein pellet was resuspended in TEAB buffer and protein concentration was determined by Pierce™ BCA Protein Assay Kit.

Equal quantities of proteins from the three PKA dKO cell lines were pooled together and 500 μg pooled protein extract was mixed with either recombinant PKA-Cα (1.5μg) or recombinant PKA-Cβ (1.5μg) enzymes obtained from Genetex Inc. (PRKACA- GTX65206-pro; PRKACB-GTX65207-pro). Samples were incubated at 30° C for 24 h in a buffer containing 50 mM Tris-HCl, 10 mM $MgCl_2$, 0.1 mM EDTA, 2 mM DTT and 250 μM ATP. Samples without any added kinases were used as controls. Following the in vitro kinase incubation, the proteins underwent a standard phosphoproteomic analysis as described previously.

Bioinformatics and data sharing. Technical replicates were summarized by taking the median value. All analyses were performed using Perseus, Excel, and R software. Moderated P-values (P_{mod}) were calculated using the empirical Bayes method, which integrates variance information from all peptides measured in the same LC-MS/MS run (10). Data have been deposited in PRIDE (as part of ProteomeXchange) with accession number PXD015050 (URL for reviewer is https://www.ebi.ac.uk/pride/archive/projects/PXD015050.)

RESULTS

Previously, the PKA-Cα-null and PKA-Cβ-null cells were characterized by immunoblotting, which showed that PKA-Cα and PKA-Cβ proteins were undetectable in the corresponding single knockout lines (9). Both single KO lines grew well and formed confluent mono-layered epithelial sheets when grown on permeable supports. Here, we used protein mass spectrometry to quantify changes in total protein abundances and changes in phosphorylation in PKA-Cα-null versus -intact, and PKA-Cβ-null versus -intact cells across the proteome.

Proteome-wide quantification of protein abundances. Quantitative data for the total abundance of all individual proteins is provided on a specially designed web page (https://hpcwebapps.cit.nih.gov/ESBL/Database/PKA-singleKO-total/) and as **Supplemental Dataset 1,** provided at https://hpcwebapps.cit.nih.gov/ESBL/Database/PKA-singleKO-total/**. Figure 2** shows changes in protein abundances corresponding to 4691 different genes in both PKA-Cα-null cells and PKA-Cβ-null cells versus their respective PKA-intact control cells. Each point shows values for a different protein. The proteins whose abundances were previously found to be significantly altered in PKA-Cα/PKA-Cβ double knockout (dKO) cells are marked by red or green points depending on the direction of change in the dKO. Interestingly, aquaporin-2 (Aqp2), which had previously been seen to be almost completely ablated in the PKA dKO cells, was decreased in only the PKA-Cα-null cells and not the PKA-Cβ-null cells. Two other proteins that were strongly decreased in abundance in the PKA dKO experiments, namely Complement Factor C3 (C3) and Mucin-4 (Muc4) were differentially affected in the two single KO cells. C3 was selectively decreased in PKA-Cα-null cells, whereas Mucin-4 was selectively decreased in PKA-Cβ-null cells. These data support the view that PKA-Cα and PKA-Cβ do not have the same physiological roles in collecting duct cells. Interestingly, PKA-Cβ was substantially increased in abundance in the PKA-Cα-null cells suggesting a compensatory response.

We plotted the changes in protein abundances in the PKA-Cα-null cells versus those in the PKA-Cβ-null cells for those proteins that changed significantly in either PKA-KO line (**Figure 3A**). As can be seen, some proteins (yellow) underwent parallel changes in abundance in both single KO cell lines, while others underwent selective, significant changes in either PKA-Cα-null (red) or PKA-Cβ-null (green) cells. Control vs. control comparisons for the same proteins are shown in **Figure 3B** illustrating the magnitude of changes expected from random variability in the mass spectrometric quantification. (The 95% confidence interval for $\log_2$(control/control**)** was 0.382). A listing of the proteins that most convincingly changed ($P_{mod} < 0.02$ and $|\log(ratio)| > 0.5$) in the PKA-Cα-null cells is given in **Table 1**, while changes in PKA-Cβ-null cells are listed in **Table 2.** Overall, we conclude that PKA-Cα and PKA-Cβ are not redundant with respect to regulation of protein abundances.

Proteome-wide quantification of protein phosphorylation. Quantitative data for all phosphopeptides are provided at (https://hpcwebapps.cit.nih.gov/ESBL/Database/PKA-singleKO-phospho/) and as **Supplemental Dataset 2**. **Figure 4** shows changes in phosphopeptide abundances (n= 4635) in both PKA-Cα-null cells and PKA-Cβ-null cells versus their respective PKA-intact (control) cells. Each point shows values for a different phosphopeptide. The phosphopeptides corresponding to previously identified PKA target sites (9) are indicated in red. Most of the PKA sites were found to be decreased in PKA-Cα-null but not in PKA-Cβ-null cells relative to controls. A listing of the phosphopeptides most convincingly changed ($P_{mod} < 0.01$ and $|\log(ratio)| > 0.5$) in the PKA-Cα-null cells is given in **Table 3**, while changes in PKA-Cβ-null cells are listed in **Table 4.** Overall, we conclude that PKA-Cα and PKA-Cβ have a substantially different set of phosphorylation targets. This difference could be due either to a difference in target sequence preference or a difference in PKA-Cα and PKA-Cβ interactomes. **Figure 5** shows the predicted target sequence preference logos for decreased single-site phosphopeptides in PKA-Cα- and PKA-Cβ-null cells, respectively. Only the PKA-Cα logo was consistent with the familiar (R/K)-(R/K)-X-p(S/T) motif generally accepted to be characteristic of PKA. Among the

82 phosphosites that were decreased in the PKA-Cβ-null cells, only four possessed the (R/K)-(R/K)-X-p(S/T) motif. The logos raise the hypothesis that the two PKA catalytic subunits may have different target sequence preferences.

In vitro phosphorylation by recombinant PKA-Cα versus PKA-Cβ. PKA-Cα and PKA-Cβ may have different target preferences. To test this hypothesis directly, we carried out in-vitro phosphorylation studies using purified recombinant PKA-Cα and PKA-Cβ catalytic subunits to phosphorylate protein extracts obtained from PKA-dKO cells. Full data are in **Supplemental Dataset 3. Figure 6A** comparing the changes in phosphorylation by PKA-Cα versus PKA-Cβ shows that both PKA catalytic subunits phosphorylate virtually identical substrates. **Figure 6B** shows that the sequence preferences for PKA-Cα versus PKA-Cβ are virtually identical. This result rules out the hypothesis that the two PKA catalytic subunits have different substrate specificities. The remaining possibility, that the two catalytic subunits have different targets because they are propinquitous to a different set of proteins, remains as the most likely explanation for the differences in targets in the intact cells.

Phosphoproteomics as a virtual proximity assay. In addition to the target sequence, another factor important to the determination of targets for a protein kinase is co-localization because a kinase can only phosphorylate a protein with which it comes into physical contact. In this sense, phosphoproteomic analysis can be viewed as a kind of large-scale proximity assay, identifying kinase/target interactions. To evaluate whether differences in PKA-Cα and PKA-Cβ phosphorylation targets result in part from differences in PKA-Cα and PKA-Cβ localization, we identified *Gene Ontology (GO-CC) Cellular Component* terms that are enriched in either set of phosphorylation targets in the intact cell experiments, relative to all proteins detected. **Table 5** shows terms enriched in phosphoproteins with altered phosphorylation in the PKA-Cα-null cells, while **Table 6** shows terms enriched in phosphoproteins with altered phosphorylation in the PKA-Cβ-null cells. Enriched terms in the PKA-Cα-null cells were largely related to cell membranes and membrane vesicles, while enriched

terms in the PKA-Cβ-null cells were related to the actin cytoskeleton and cell junctions, suggesting that in vivo cellular subdomains of the PKA-Cα and PKA-Cβ differ.

PKA-Cα and PKA-Cβ regulate different protein kinases. Many phosphorylation sites that changed in the PKA-Cα-null or PKA-Cβ-null cells did not conform to the classic PKA target motif and presumably undergo changes in phosphorylation as a result of secondary effects on other protein kinases. **Table 7** shows protein kinase catalytic proteins that underwent changes in phosphorylation in either the PKA-Cα- or PKA-Cβ-null cells. Many of the altered phosphorylation sites have known effects on enzyme activity as indicated in the last column. The affected kinases, namely calcium/calmodulin-dependent protein kinase kinase 2 (Camkk2), the epidermal growth factor receptor kinase (Egfr), myosin light chain kinase (Mylk), p21-activated kinase (Pak2), AMP-activated protein kinase α-1 (Prkaa1), and salt-inducible kinase 2 (Sik2), all underwent changes in phosphorylation in response to PKA-Cα deletion, while only Egfr underwent a change in phosphorylation in response to PKA-Cβ deletion. This supports the conclusion that PKA-Cα or PKA-Cβ have different downstream signaling networks.

Differential regulation of cAMP signaling proteins by PKA-Cα and PKA-Cβ. One factor involved in localization of protein kinase A in the cell is its interaction with anchoring proteins such as AKAPs. **Table 8** shows altered phosphopeptides belonging to AKAP proteins or proteins with GO terms containing “cAMP” or “cyclic-AMP” to identify possible other AKAP interactors. Among the phosphoproteins in this list are Akap1, Akap12, cAMP phosphodiesterase 4C (Pde4c), cAMP phosphodiesterase 7A (Pde7a), AMP-activated protein kinase α-1 (Prkaa1), as well as two PKA regulatory subunits, RIα (Prkar1a) and RIIβ (Prkar2b). All of these (except for one site in Akap12) underwent changes in response to PKA-Cα deletion but not PKA-Cβ deletion. Thus, the phosphorylation evidence suggests that PKA-Cα interacts more extensively with components of AKAP complexes than does PKA-Cβ, at least with regard to phosphorylation.

An important role of vasopressin-signaling in renal collecting duct cells is transcriptional regulation, particularly regulation of transcription of the *Aqp2* gene. **Table 9** shows transcription factors with altered phosphorylation in PKA-Cα-null or PKA-Cβ-null cells. Among all transcription factors, 241 phosphopeptides were quantified. There were 14 phosphopeptides that were substantially changed in abundance in 13 different transcription factor proteins. Most of the altered sites had proline in position +1 relative to the phosphorylated S or T, signifying altered phosphorylation by protein kinases in the cyclin-dependent kinase or MAP kinase families. Only one transcription factor underwent differential phosphorylation at a site with the (R/K)-(R/K)-X-p(S/T) motif, namely "cyclic AMP-dependent transcription factor ATF-7", which showed a marked decrease in phosphorylation in the PKA-Cα-null but not the PKA-Cβ-null cells. Atf7 is a b-ZIP transcription factor that is inactive as a homodimer but can transactivate genes when heterodimerized with members of the AP-1 family including Jund (6), which underwent a decrease in phosphorylation. Beyond the transcription factors, various transcriptional co-regulators may participate in vasopressin-mediated regulation of transcription. One such protein is β-catenin, which shows increased phosphorylation at S552, a PKA target site (9), in response to vasopressin. Interestingly, S552 of β-catenin showed a marked decrease in phosphorylation in the PKA-Cα-null cells, but not the PKA-Cβ-null cells (**Table 3**). In general, as with other categories of proteins, changes in phosphorylation of transcription factors and their coregulators are different in PKA-Cα-null or PKA-Cβ-null cells, again supporting the conclusion that the two PKA catalytic subunits fulfill different cellular functions.

DISCUSSION

Based on the observations in this paper, we conclude that PKA-Cα and PKA-Cβ do not have redundant functions. Indeed, while some overlap exists between the two in terms of phosphorylation targets, large differences were seen at a whole phosphoproteome level. PKA-Cα-null cells showed decreased phosphorylation dominated by sites with the classical PKA motif, viz. (R/K)-(R/K)-X-p(S/T), while only very few of the decreased phosphorylation sites in the PKA-Cβ-null cells contained this motif. However, in vitro incubation with recombinant PKA-Cα and PKA-Cβ resulted in phosphorylation of virtually identical sites, with a predominance of the (R/K)-(R/K)-X-p(S/T) motif. A key question is, "If the catalytic regions of PKA-Cα and PKA-Cβ have nearly identical in vitro target specificities, why is there such a difference in phosphorylation targets in the intact cells?". The question was addressed by the bioinformatics analysis of phosphorylation targets, showing that completely different *Gene Ontology Cellular Component* terms are associated with the two sets of phosphorylation targets. Specifically, PKA-Cα targets were largely related to cell membranes and membrane vesicles, while PKA-Cβ targets were related to the actin cytoskeleton and cell junctions, indicating that PKA-Cα and PKA-Cβ interact with different sets of proteins in cells. This difference could arise from differences in the non-catalytic regions of the two kinases that result in a different set of local interactions with potential substrates.

One possibility is that the two catalytic subunits could interact with different AKAPs and/or PKA regulatory subunits (15). Phosphoproteomic results point to a preferential association of PKA-Cα with the regulatory R2 β subunit (Prkar2b), which showed a marked decrease at S112 in the PKA-Cα null cells but not the PKA-Cβ null cells **(Table 8)**. The second possibility is that there could be differential interactions with so-called C-kinase anchoring proteins (C-KAPs) (25). The third possibility is that there may be a difference in protein-protein interactions with PDZ domain-containing proteins (1). PKA-Cα contains a class-1 carboxy terminal PDZ-ligand motif (–TxF), while PKA-Cβ, ends with –CxF which does not conform to a PDZ ligand motif. In previous studies (3), we showed that vasopressin treatment of

native inner medullary collecting duct cells results in increased phosphorylation of several PDZ domain-containing proteins (connector enhancer of kinase suppressor of Ras 3 (Cnksr3), PDZ domain-containing protein GIPC1 (Gipc1), multiple-PDZ domain protein (Mpdz), and PDZ and LIM domain protein-5 (Pdlim5). That paper showed that proteins with class I COOH-terminal 3-amino acid motifs are more likely to show increases in phosphorylation in response to vasopressin than proteins without the motif.

In addition to phosphorylation differences, PKA-Cα and PKA-Cβ deletions resulted in many differences in what proteins underwent changes in total protein abundances. Thus, in terms of regulation of protein abundances, PKA-Cα and PKA-Cβ proteins appear to have non-redundant functions. For example, AQP2 was markedly decreased in PKA-Cα-null cells but not in PKA-Cβ-null cells. This result suggests that PKA-Cα is the predominant catalytic subunit responsible for the regulation of AQP2 abundance. Similarly, complement component C3 was markedly decreased in PKA-Cα-null cells but not in PKA-Cβ-null cells. In contrast, the abundance of mucin-4 (Muc4) was substantially decreased in PKA-Cβ-null cells but not in PKA-Cα-null cells. Prior studies in mpkCCD cells have shown that, in the PKA double knockout cells AQP2, C3, and Muc4 mRNA and protein levels were markedly decreased (9).

Data resource. In addition to the scientific findings highlighted above, this paper provides added value in the form of two web resources that allow users to interrogate data from this paper. These resources have been included with other phosphoproteomic data on the *Kidney Systems Biology* Project website (https://hpcwebapps.cit.nih.gov/ESBL/Database/).

REFERENCES

1. **Colledge M, Dean RA, Scott GK, Langeberg LK, Huganir RL, and Scott JD**. Targeting of PKA to glutamate receptors through a MAGUK-AKAP complex. *Neuron* 27: 107-119, 2000.
2. **Cox J, and Mann M**. MaxQuant enables high peptide identification rates, individualized p.p.b.-range mass accuracies and proteome-wide protein quantification. *Nat Biotechnol* 26: 1367-1372, 2008.
3. **Deshpande V, Kao A, Raghuram V, Datta A, Chou CL, and Knepper MA**. Phosphoproteomic identification of vasopressin V2 receptor-dependent signaling in the renal collecting duct. *Am J Physiol Renal Physiol* 317: F789-F804, 2019.
4. **Fenton RA, Murali SK, and Moeller HB**. Advances in Aquaporin-2 trafficking mechanisms and their implications for treatment of water balance disorders. *Am J Physiol Cell Physiol* 2020.
5. **Fushimi K, Uchida S, Hara Y, Hirata Y, Marumo F, and Sasaki S**. Cloning and expression of apical membrane water channel of rat kidney collecting tubule. *Nature* 361: 549-552, 1993.
6. **Hai T, and Curran T**. Cross-family dimerization of transcription factors Fos/Jun and ATF/CREB alters DNA binding specificity. *Proc Natl Acad Sci U S A* 88: 3720-3724, 1991.
7. **Hasler U, Mordasini D, Bens M, Bianchi M, Cluzeaud F, Rousselot M, Vandewalle A, Feraille E, and Martin PY**. Long term regulation of aquaporin-2 expression in vasopressin-responsive renal collecting duct principal cells. *J Biol Chem* 277: 10379-10386, 2002.
8. **Hasler U, Nielsen S, Feraille E, and Martin PY**. Posttranscriptional control of aquaporin-2 abundance by vasopressin in renal collecting duct principal cells. *Am J Physiol Renal Physiol* 290: F177-187, 2006.
9. **Isobe K, Jung HJ, Yang CR, Claxton J, Sandoval P, Burg MB, Raghuram V, and Knepper MA**. Systems-level identification of PKA-dependent signaling in epithelial cells. *Proc Natl Acad Sci U S A* 114: E8875-E8884, 2017.
10. **Kammers K, Cole RN, Tiengwe C, and Ruczinski I**. Detecting Significant Changes in Protein Abundance. *EuPA Open Proteom* 7: 11-19, 2015.
11. **Katsura T, Gustafson CE, Ausiello DA, and Brown D**. Protein kinase A phosphorylation is involved in regulated exocytosis of aquaporin-2 in transfected LLC-PK1 cells. *Am J Physiol* 272: F817-822, 1997.
12. **Klussmann E, Maric K, Wiesner B, Beyermann M, and Rosenthal W**. Protein kinase A anchoring proteins are required for vasopressin-mediated translocation of aquaporin-2 into cell membranes of renal principal cells. *J Biol Chem* 274: 4934-4938, 1999.
13. **Limbutara K, Kelleher A, Yang CR, Raghuram V, and Knepper MA**. Phosphorylation Changes in Response to Kinase Inhibitor H89 in PKA-Null Cells. *Sci Rep* 9: 2814, 2019.
14. **Matsumura Y, Uchida S, Rai T, Sasaki S, and Marumo F**. Transcriptional regulation of aquaporin-2 water channel gene by cAMP. *J Am Soc Nephrol* 8: 861-867, 1997.
15. **Michel JJ, and Scott JD**. AKAP mediated signal transduction. *Annu Rev Pharmacol Toxicol* 42: 235-257, 2002.
16. **Navarrete-Perea J, Yu Q, Gygi SP, and Paulo JA**. Streamlined Tandem Mass Tag (SL-TMT) Protocol: An Efficient Strategy for Quantitative (Phospho)proteome Profiling Using Tandem Mass Tag-Synchronous Precursor Selection-MS3. *J Proteome Res* 17: 2226-2236, 2018.
17. **Nedvetsky PI, Tabor V, Tamma G, Beulshausen S, Skroblin P, Kirschner A, Mutig K, Boltzen M, Petrucci O, Vossenkamper A, Wiesner B, Bachmann S, Rosenthal W, and Klussmann E**. Reciprocal regulation of aquaporin-2 abundance and degradation by protein kinase A and p38-MAP kinase. *J Am Soc Nephrol* 21: 1645-1656, 2010.
18. **Nielsen S, Chou CL, Marples D, Christensen EI, Kishore BK, and Knepper MA**. Vasopressin increases water permeability of kidney collecting duct by inducing translocation of aquaporin-CD water channels to plasma membrane. *Proc Natl Acad Sci U S A* 92: 1013-1017, 1995.

19. **Nishimoto G, Zelenina M, Li D, Yasui M, Aperia A, Nielsen S, and Nairn AC**. Arginine vasopressin stimulates phosphorylation of aquaporin-2 in rat renal tissue. *Am J Physiol* 276: F254-259, 1999.
20. **Olesen ET, and Fenton RA**. Aquaporin-2 membrane targeting: still a conundrum. *Am J Physiol Renal Physiol* 312: F744-F747, 2017.
21. **Procino G, Carmosino M, Marin O, Brunati AM, Contri A, Pinna LA, Mannucci R, Nielsen S, Kwon TH, Svelto M, and Valenti G**. Ser-256 phosphorylation dynamics of Aquaporin 2 during maturation from the ER to the vesicular compartment in renal cells. *FASEB J* 17: 1886-1888, 2003.
22. **Roos KP, Strait KA, Raphael KL, Blount MA, and Kohan DE**. Collecting duct-specific knockout of adenylyl cyclase type VI causes a urinary concentration defect in mice. *Am J Physiol Renal Physiol* 302: F78-84, 2012.
23. **Salhadar K, Matthews A, Raghuram V, Limbutara K, Yang CR, Datta A, Chou CL, and Knepper MA**. Phosphoproteomic Identification of Vasopressin/cAMP/PKA-Dependent Signaling in Kidney. *Mol Pharmacol* 2020.
24. **Sandoval PC, Claxton JS, Lee JW, Saeed F, Hoffert JD, and Knepper MA**. Systems-level analysis reveals selective regulation of Aqp2 gene expression by vasopressin. *Sci Rep* 6: 34863, 2016.
25. **Soberg K, and Skalhegg BS**. The Molecular Basis for Specificity at the Level of the Protein Kinase a Catalytic Subunit. *Front Endocrinol (Lausanne)* 9: 538, 2018.
26. **UniProt Consortium T**. UniProt: the universal protein knowledgebase. *Nucleic Acids Res* 46: 2699, 2018.

ACKNOWLEDGEMENTS

This work was funded by the Division of Intramural Research, National Heart, Lung, and Blood Institute (projects ZIA-HL001285 and ZIA- HL006129, MAK). Karim Salhadar was a member of the Biomedical Engineering Student Internship Program (BESIP, Robert Lutz, Director) supported by the National Institute for Biomedical Imaging and Bioengineering (June-August 2018). Mass spectrometry utilized the NHLBI Proteomics Core Facility (M. Gucek, Director). Supplemental data are deposited at https://hpcwebapps.cit.nih.gov/ESBL/Database/Supplemental_Data_PKA_sKO/.

Author Contributions

V.R., and M.A.K., developed the concept and designed the experiments. V.R., K.S, E.P., and C-R.Y., performed the experiments. V.R., K.L., and M.A.K., analyzed the data. V.R., K.L., C-R.Y., and M.A.K interpreted the results of the experiments. V.R., K.S., K.L., and M.A.K., drafted the manuscript and prepared figures. All authors edited, revised, and reviewed the manuscript.

Competing interests

The author(s) declare no competing interests.

Data availability

The mass spectrometry proteomics data have been deposited to the ProteomeXchange Consortium via the PRIDE partner repository with the dataset accession number PXD015050 (URL for reviewer is https://www.ebi.ac.uk/pride/archive/projects/PXD015050.

FIGURE LEGENDS

Figure 1. Experimental method. Cells were grown on permeable supports with three biological replicates as indicated. There were two technical replicates each resulting in a total of 24 samples. Proteins were isolated, trypsinized and labeled using isotopic tags (TMT-11 plex). The 24 samples were combined into three batches of 8 each with a shared sample pooled from all 24 samples. The combined samples were processed for proteomic and phosphoproteomic analysis as described in Methods.

Figure 2. Effect of PKA-Cα (left) and PKA-Cβ (right) deletion on protein abundances in mouse mpkCCD cells. Red points indicate proteins decreased in PKA-Cα/PKA-Cβ double knockout cells (9). Green points indicate proteins increased in PKA-Cα/PKA-Cβ double knockout cells (9). Arrows to these red and green points show official gene symbols for the specific proteins.

Figure 3. Comparison of effects of PKA-Cα and PKA-Cβ deletion on protein abundances. A. Red points show proteins changed with PKA-Cα deletion, but not PKA-Cβ deletion. Green points show proteins changed with PKA-Cβ deletion, but not PKA-Cα deletion. Yellow points are changed in both, but not necessarily in the same direction. B. Intrinsic variability of the data estimated by comparing values for PKA-intact controls versus other controls (see text).

Figure 4. Effect of PKA-Cα (left) and PKA-Cβ (right) deletion on phosphopeptide abundances in mouse mpkCCD cells. Red points indicate phosphorylation sites altered in PKA-Cα/PKA-Cβ double knockout cells (9). Arrows to these red points show official gene symbol and amino acid number of phosphorylated site for those sites above P_{mod} threshold (-log P_{mod} > 1.3).

Figure 5. **Sequence preference logos from sites decreased with PKA-Cα deletion (top) and PKA-Cβ deletion (bottom**). Logos were generated using *PTM-Logo* with a background of all unchanged phosphopeptides.

Figure 6. Results of *in vitro* phosphorylation experiments. Protein extracts from PKA double knockout cells (PKA-Cα and PKA-Cβ) were incubated with recombinant PKA-Cα or PKA-Cβ and phosphorylation was quantified by mass spectrometry. A. There was a marked similarity between responses to the two recombinant kinase proteins. B. Sequence preference logos derived from the analysis were almost identical.

Figure 1

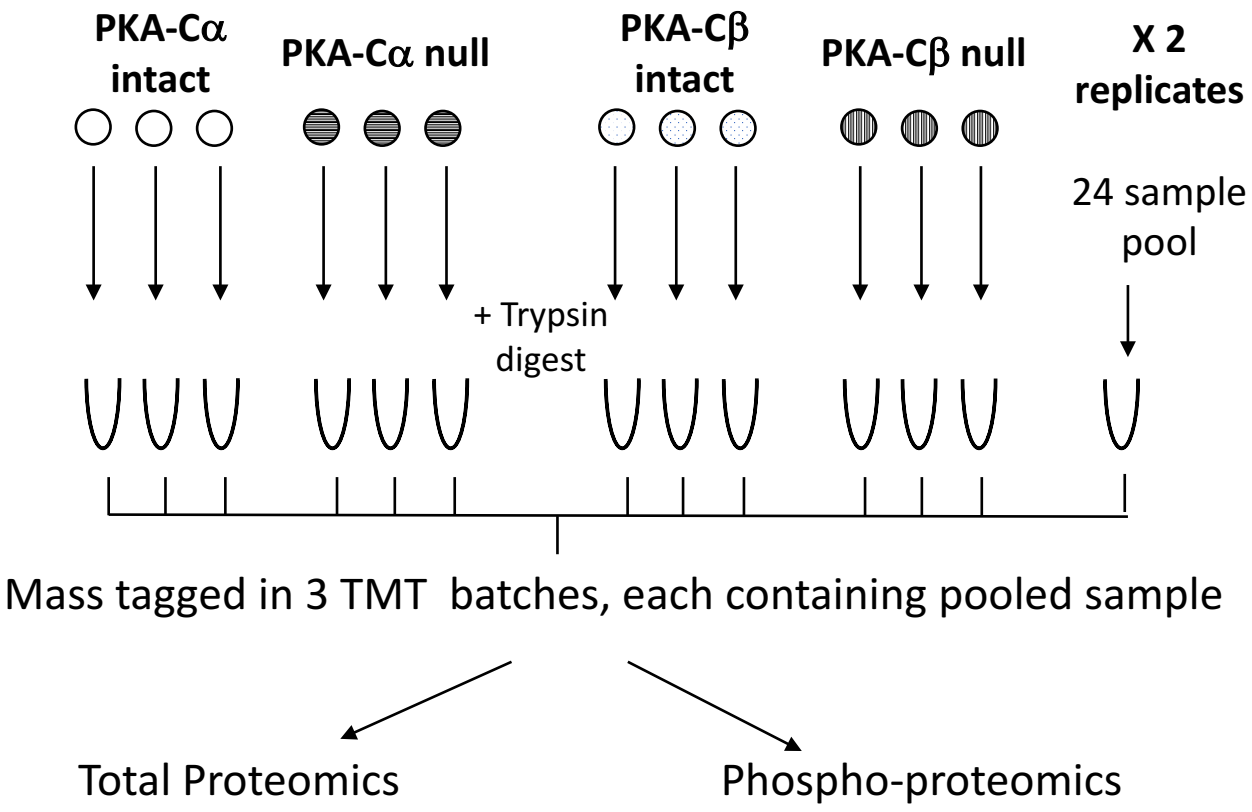

Figure 1. Experimental method. Cells were grown on permeable supports with three biological replicates as indicated. There were two technical replicates each resulting in a total of 24 samples. Proteins were isolated, trypsinized and labeled using isotopic tags (TMT-11 plex). The 24 samples were combined into three batches of 8 each with a shared sample pooled from all 24 samples. The combined samples were processed for proteomic and phosphoproteomic analysis as described in Methods.

Figure 2

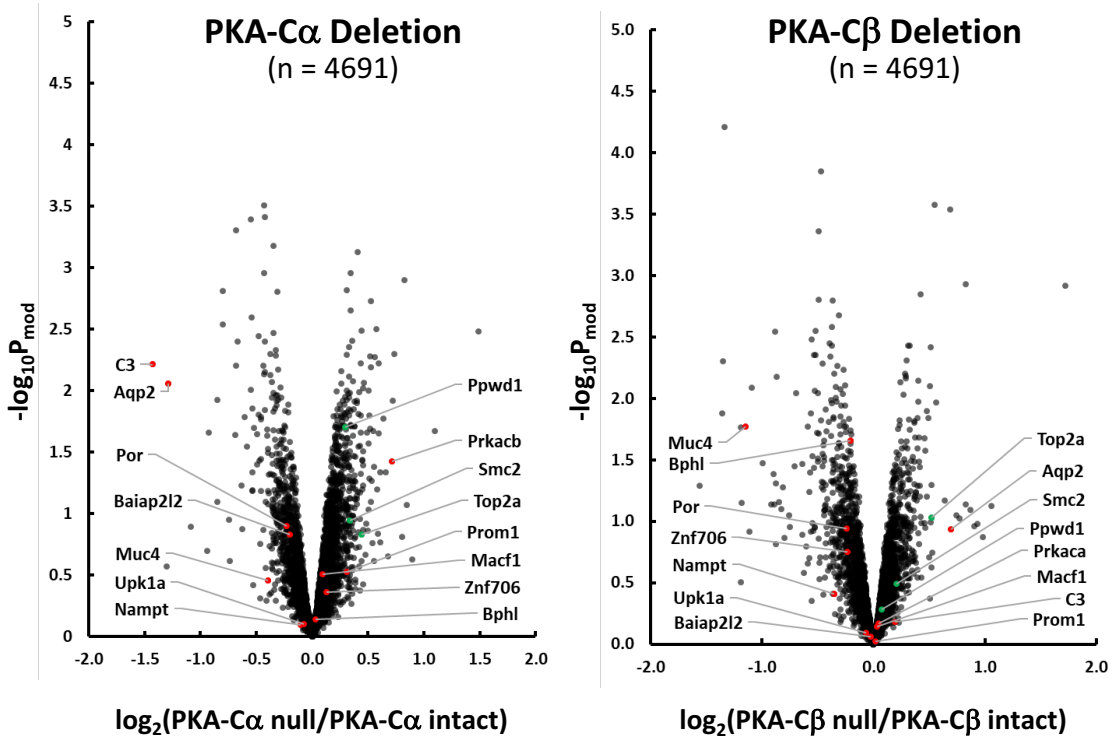

Figure 2. Effect of PKA-Ca (left) and PKA-Cb (right) deletion on protein abundances in mouse mpkCCD cells. Red points indicate proteins decreased in PKA-Ca/PKA-Cb double knockout cells (8). Green points indicate proteins increased in PKA-Ca/PKA-Cb double knockout cells (8). Arrows to these red and green pints show official gene symbols for the specific proteins.

Figure 3

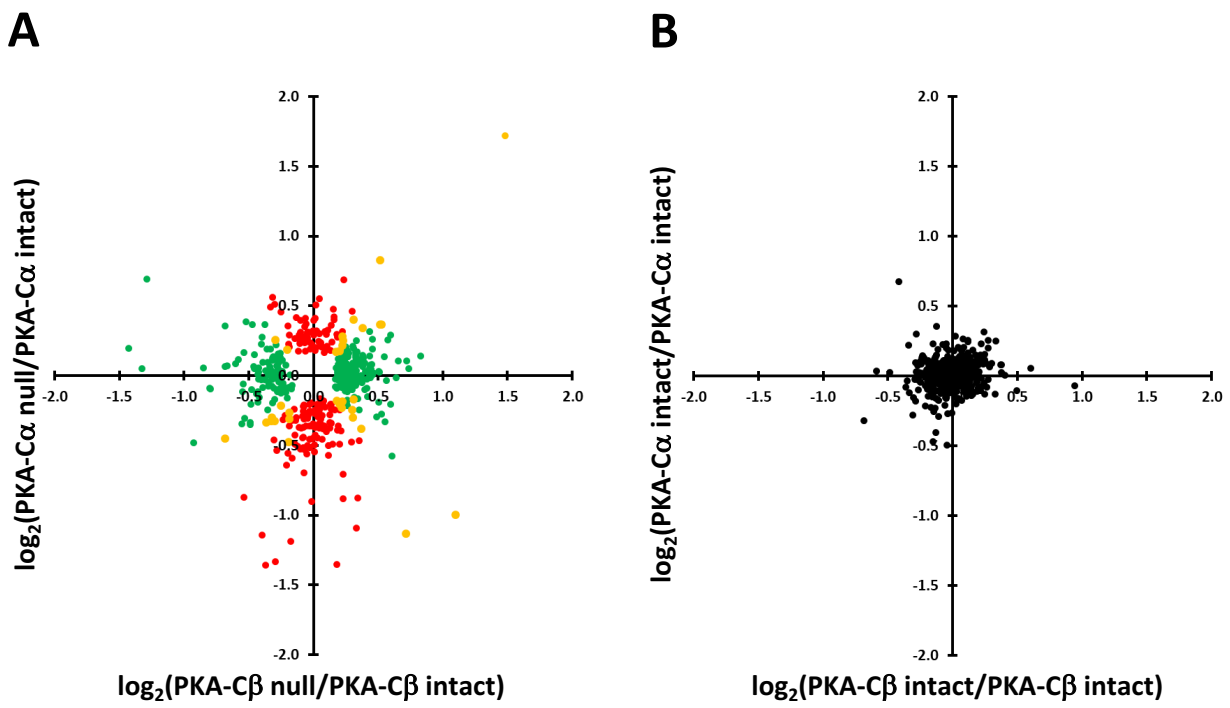

Figure 3. Comparison of effects of PKA-Cα and PKA-Cβ deletion on protein abundances. A. Red points show proteins changed with PKA-Cα deletion, but not PKA-Cβ deletion. Green points show proteins changed with PKA-Cβ deletion, but not PKA-Cα deletion. Yellow points are changed in both, but not necessarily in the same direction. B. Intrinsic variability of the data estimated by comparing values for PKA-intact controls versus other controls (see text).

Figure 4

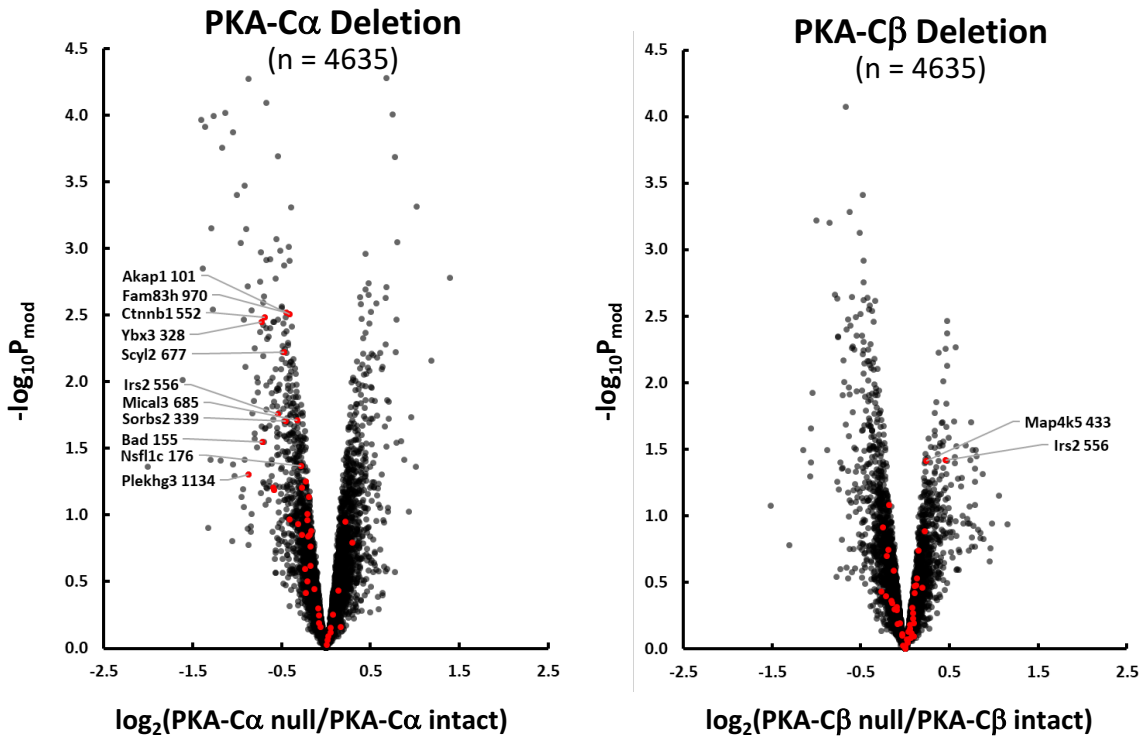

Figure 4. Effect of PKA-Cα (left) and PKA-Cβ (right) deletion on phosphopeptide abundances in mouse mpkCCD cells. Red points indicate phosphorylation sites altered in PKA-Cα/PKA-Cβ double knockout cells (8). Arrows to these red points show official gene symbol and amino acid number of phosphorylated site for those sites above P_{mod} threshold (-log P_{mod} > 1.3).

Figure 5

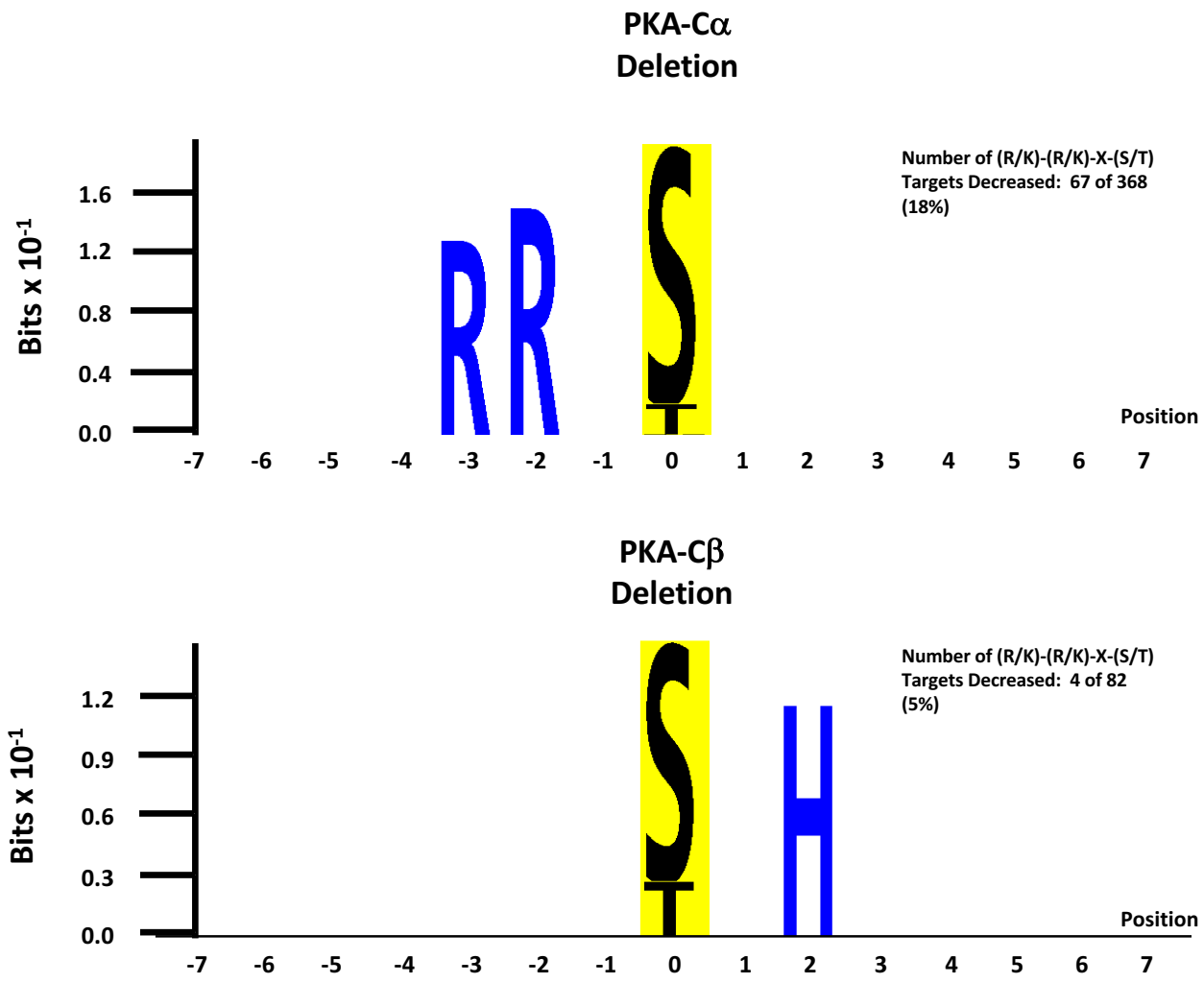

Figure 5. **Sequence preference logos from sites decreased with PKA-Cα deletion (top) and PKA-Cβ deletion (bottom**). Logos were generated using *PTM-Logo* with a background of all unchanged phosphopeptides.

Figure 6

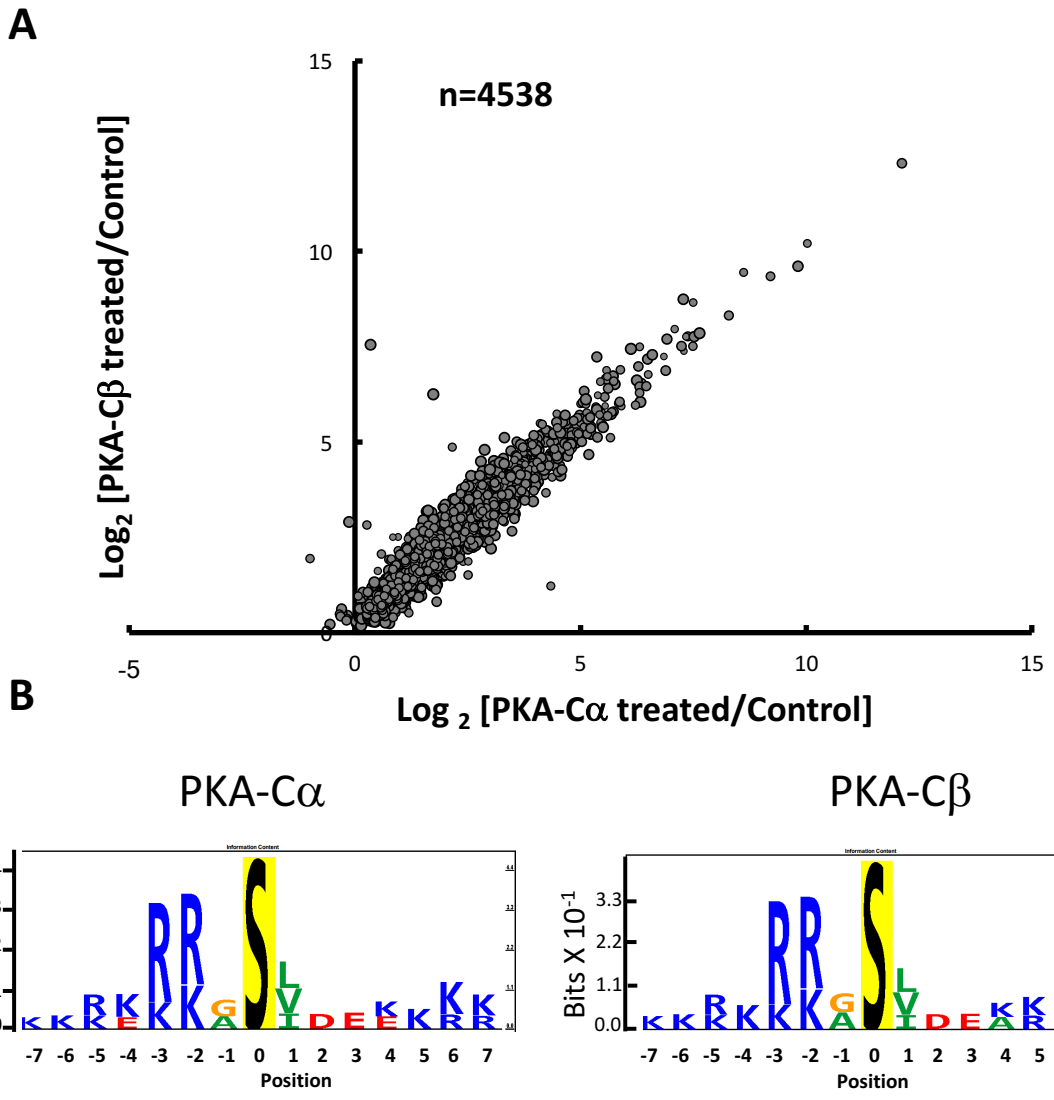

Figure 6. Results of *in vitro* phosphorylation experiments. Protein extracts from PKA double knockout cells (PKA-Cα and PKA-Cβ) were incubated with recombinant PKA-Cα or PKA-Cβ and phosphorylation was quantified by mass spectrometry. A. There was a marked similarity between responses to the two recombinant kinase proteins. B. Sequence preference logos derived from the analysis were almost identical.

Table 1. Proteins with substantial changes in abundance in response to PKA-Cα deletion (P_{mod} < 0.02 and |log(ratio)| > 0.5).

UniProt ID	Gene Symbol	Annotation	Log_2 (PKA-Cα null/ PKA-Cα intact)	Pmod	Log_2 (PKA-Cβ null/ PKA-Cβ intact)	Pmod	Log_2 (PKA-Cα null/ PKA-Cβ null)
P01027	**C3**	Complement C3	**-1.427**	0.006	0.195	0.655	-0.990
P56402	**Aqp2**	Aquaporin-2	**-1.286**	0.009	0.694	0.115	-1.520
Q9QYI5	**Dnajb2**	DnaJ homolog subfamily B member 2	**-0.850**	0.012	0.056	0.848	-0.513
P97742	**Cpt1a**	Carnitine O-palmitoyltransferase 1, liver isoform	**-0.799**	0.002	-0.091	0.647	-0.467
Q8BH86	**Dglucy**	D-glutamate cyclase, mitochondrial	**-0.798**	0.003	-0.094	0.666	-0.090
P24472	**Gsta4**	Glutathione S-transferase A4	**-0.684**	0.006	-0.451	0.049	0.199
Q9EPK8	**Trpv4**	Transient receptor potential channel subfamily V member 4	**-0.682**	4.93E-04	0.067	0.647	-0.435
Q9WTQ5	**Akap12**	A-kinase anchor protein 12	**-0.669**	0.004	0.070	0.714	-0.379
Q99J39	**Mlycd**	Malonyl-CoA decarboxylase, mitochondrial	**-0.602**	0.016	0.087	0.690	-0.245
Q8BLF1	**Nceh1**	Neutral cholesterol ester hydrolase 1	**-0.551**	0.010	-0.346	0.077	0.072
P63011	**Rab3a**	Ras-related protein Rab-3A	**-0.550**	4.05E-04	-0.115	0.324	-0.186
P26443	**Glud1**	Glutamate dehydrogenase 1, mitochondrial	**-0.543**	0.003	-0.057	0.692	-0.376
G3X9Y6	**Akr1c19**	Aldo-keto reductase family 1, member C19	**-0.534**	0.014	-0.307	0.123	-0.086
Q8BG05	**Hnrnpa3**	Heterogeneous nuclear ribonucleoprotein A3	**0.507**	0.010	0.033	0.845	0.162
D3YYU8	**Obsl1**	Obscurin-like protein 1	**0.512**	0.016	0.024	0.897	0.332
P62482	**Kcnab2**	Voltage-gated potassium channel subunit beta-2	**0.518**	0.005	0.366	0.033	0.062
Q8VI84	**Noc3l**	Nucleolar complex protein 3 homolog	**0.524**	0.002	0.369	0.016	0.029
Q5DU09	**Znf652**	Zinc finger protein 652	**0.527**	0.006	-0.275	0.108	0.396
O88508	**Dnmt3a**	DNA (cytosine-5)-methyltransferase 3A	**0.562**	0.005	-0.034	0.838	0.198
O54786	**Dffa**	DNA fragmentation factor subunit alpha	**0.576**	0.003	0.255	0.127	0.270
Q9D187	**Ciao2b**	Cytosolic iron-sulfur assembly component 2B	**0.596**	0.006	-0.206	0.268	0.422
Q61180	**Scnn1a**	Amiloride-sensitive sodium channel subunit alpha	**0.637**	0.017	-0.016	0.945	0.616
P0DOV2	**Ifi204**	Interferon-activable protein 204	**0.722**	0.012	0.108	0.664	0.224
Q9JK42	**Pdk2**	Pyruvate dehydrogenase kinase isozyme 2	**0.734**	0.005	0.049	0.821	0.167
P26645	**Marcks**	Myristoylated alanine-rich C-kinase substrate	**1.486**	0.003	1.718	0.001	0.089
P05132	**Prkaca**	cAMP-dependent protein kinase catalytic subunit α	**-**	**-**	0.049	0.677	-

Table 2. Proteins with substantial changes in abundance in response to PKA-Cβ deletion (P_{mod} < 0.02 and |log(ratio)| > 0.5).

UniProt ID	Gene Symbol	Annotation	Log_2 (PKA-Cα null/ PKA-Cα intact)	Pmod	Log_2 (PKA-Cβ null/ PKA-Cβ intact)	Pmod	Log_2 (PKA-Cα null/ PKA-Cβ null)
Q8VCT4	**Ces1d**	Carboxylesterase 1D	-0.370	0.440	**-1.358**	0.013	0.731
Q8CEZ4	**Mab21l4**	Protein mab-21-like 4	0.180	0.652	**-1.351**	0.005	1.130
P30115	**Gsta3**	Glutathione S-transferase A3	-0.294	0.202	**-1.334**	6.23E-05	1.129
P08074	**Cbr2**	Carbonyl reductase [NADPH] 2	-0.178	0.683	**-1.186**	0.017	0.686
Q8JZM8	**Muc4**	Mucin-4	-0.396	0.353	**-1.144**	0.017	0.696
P00329	**Adh1**	Alcohol dehydrogenase 1	0.334	0.348	**-1.094**	0.008	1.375
Q7TPW1	**Nexn**	Nexilin	0.228	0.349	**-0.881**	0.003	0.724
Q9D939	**Sult1c2**	Sulfotransferase 1C2	-0.535	0.065	**-0.869**	0.007	0.643
Q62469	**Itga2**	Integrin alpha-2	-0.074	0.743	**-0.696**	0.009	0.684
Q99LB7	**Sardh**	Sarcosine dehydrogenase, mitochondrial	-0.163	0.457	**-0.591**	0.017	0.530
Q9WUU7	**Ctsz**	Cathepsin Z	-0.053	0.786	**-0.562**	0.013	0.585
Q8R3G9	**Tspan8**	Tetraspanin-8	-0.199	0.212	**-0.557**	0.003	0.446
P22935	**Crabp2**	Cellular retinoic acid-binding protein 2	-0.282	0.088	**-0.534**	0.004	0.120
P63082	**Atp6v0c**	V-type proton ATPase 16 kDa proteolipid subunit	-0.101	0.556	**-0.526**	0.009	0.401
Q80V42	**Cpm**	Carboxypeptidase M	-0.077	0.607	**-0.516**	0.004	0.408
P12265	**Gusb**	Beta-glucuronidase	-0.032	0.819	**-0.516**	0.003	0.496
P17563	**Selenbp1**	Methanethiol oxidase	-0.122	0.525	**-0.506**	0.019	0.228
Q5FWI3	**Cemip2**	Cell surface hyaluronidase	0.020	0.899	**0.508**	0.008	0.281
P55264	**Adk**	Adenosine kinase	-0.297	0.059	**0.513**	0.004	-0.689
Q99PT3	**Ino80b**	INO80 complex subunit B	0.048	0.658	**0.551**	2.66E-04	-0.279
Q8K0C4	**Cyp51a1**	Lanosterol 14-alpha demethylase	-0.313	0.117	**0.563**	0.011	-0.479
P28661	**Septin4**	Septin-4	0.235	0.106	**0.690**	2.90E-04	-0.229
Q80Z25	**Ofd1**	Oral-facial-digital syndrome 1 protein homolog	0.518	0.020	**0.826**	0.001	-0.008
P26645	**Marcks**	Myristoylated alanine-rich C-kinase substrate	1.486	0.003	**1.718**	0.001	0.089
P68181	**Prkacb**	cAMP-dependent protein kinase catalytic subunit beta	0.717	0.038	-	-	-

Table 3. Phosphopeptides most convincingly changed in PKA-Cα-null cells versus PKA-Cα-intact (P_{mod} < 0.01 and |log(ratio)| > 0.5). PKA-Cβ-null data for the same peptides is also given for comparison.

UniProt ID	Gene Symbol†	Amino acid number	Annotation	Sequence	Log_2 (PKA-Cα null/ PKA-Cα intact)	P_{mod}	Log_2 (PKA-Cβ null/ PKA-Cβ intact)	P_{mod}
P16254	**Srp14**	44	Signal recognition particle 14 kDa protein	KS*SVEGLEPAENK	**-1.41**	**1.09E-04**	0.18	0.472
P31324	**Prkar2b**	112	cAMP-dependent protein kinase type II-beta regulatory subunit	RAS*VCAEAYNPDEEEDDAESR	**-1.38**	**0.001**	-0.29	0.402
P05213	**Tuba1b; Tuba4a; Tuba1a; Tuba3a; Tuba1c**	158	Tubulin alpha-1B chain; Tubulin alpha-4A chain; Tubulin alpha-1A chain; Tubulin alpha-1C chain	LS*VDYGK	**-1.36**	**1.21E-04**	0.28	0.266
E9PVZ8	**Golgb1**	2655	Golgi autoantigen, golgin subfamily b, macrogolgin 1	KVS*EIEDQLK	**-1.29**	**0.001**	0.20	0.484
Q68FG2	**Sptbn2**	2254	Spectrin beta chain	RGS*LGFYK	**-1.28**	**0.003**	0.20	0.576
P16254	**Srp14**	44	Signal recognition particle 14 kDa protein	KS*SVEGLEPAENK	**-1.27**	**1.02E-04**	0.25	0.276
P14152	**Mdh1**	241	Malate dehydrogenase, cytoplasmic	KLS*SAMSAAK	**-1.17**	**1.75E-04**	0.07	0.768
Q9ES28	**Arhgef7**	830	Rho guanine nucleotide exchange factor 7	S*LEEEQR	**-1.13**	**9.54E-05**	0.18	0.371
Q9DBC7	**Prkar1a**	83	cAMP-dependent protein kinase type I-alpha regulatory subunit	EDEIS*PPPPNPVVK	**-1.05**	**1.34E-04**	-0.09	0.642
G3X9K3	**Arfgef1**	1076	Brefeldin A-inhibited guanine nucleotide-exchange protein 1	EGS*LTGTK	**-0.96**	**0.001**	0.09	0.688
Q9CZX9	**Emc4**	36	ER membrane protein complex subunit 4	SDRGS*GQGDSLYPVGYLDK	**-0.93**	**0.003**	0.18	0.485
Q8CI52	**Gramd1c**	532	Protein Aster-C	SS*TDLGFEAK	**-0.92**	**3.38E-04**	-0.04	0.832
Q91XA2	**Golm1**	299	Golgi membrane protein 1	PEEDS*QYPER	**-0.91**	**0.008**	0.08	0.794
Q9DBC7	**Prkar1a**	83	cAMP-dependent protein kinase type I-alpha regulatory subunit	TDSREDEIS*PPPPNPVVK	**-0.90**	**0.001**	-0.11	0.599
Q8CHT1	**Ngef**	84	Ephexin-1	RAS*DQADLPK	**-0.88**	**0.002**	0.32	0.179
Q8CI52	**Gramd1c**	531	Protein Aster-C	S*STDLGFEAK	**-0.87**	**5.31E-05**	0.08	0.558
P43277	**Hist1h1c; Hist1h1d**	37	Histone H1.2; Histone H1.3	KAS*GPPVSELITK	**-0.84**	**0.003**	0.26	0.263
Q8C341	**Suco**	1069	SUN domain-containing ossification factor	RTS*FPLIR	**-0.80**	**0.006**	0.13	0.597
Q8K4L3	**Svil**	857	Supervillin	KLS*VDNNTSATDYK	**-0.77**	**0.009**	-0.03	0.918
Q67FY2	**Bcl9l**	118	B-cell CLL/lymphoma 9-like protein	SVS*VDSGEQR	**-0.75**	**0.002**	-0.86	0.001

F6ZDS4	**Tpr**	2204	Nucleoprotein TPR	TVPS*TPTLVVPHR	**-0.74**	**0.004**	-0.47	0.047
Q8C079	**Strip1**	59	Striatin-interacting protein 1	KDS*EGYSESPDLEFEYADTDK	**-0.73**	**0.001**	0.08	0.642
Q9JKB3	**Ybx3**	328	Y-box-binding protein 3	S*RPLNAVSQDGK	**-0.72**	**0.004**	0.09	0.644
Q6NZF1	**Zc3h11a**	740	Zinc finger CCCH domain-containing protein 11A	RLS*SASTGKPPLSVEDDFEK	**-0.71**	**0.006**	-1.00	0.001
O35609	**Scamp3**	78	Secretory carrier-associated membrane protein 3	KLS*PTEPR	**-0.71**	**0.004**	0.18	0.389
P15066	**Jund; Jun**	100	Transcription factor jun-D	LAS*PELER	**-0.69**	**0.002**	0.07	0.720
Q02248	**Ctnnb1**	552	Catenin beta-1	RTS*M^GGTQQQFVEGVR	**-0.69**	**0.003**	-0.15	0.455
Q8BUH8	**Senp7**	12	Sentrin-specific protease 7	RAS*SEIVTEGK	**-0.67**	**8.08E-05**	-0.67	8.49E-05
Q6PGG2	**Gmip**	260	GEM-interacting protein	S*REEAQAK	**-0.67**	**0.001**	0.33	0.057
Q04899	**Cdk18**	75	Cyclin-dependent kinase 18	RLS*LPMDIR	**-0.66**	**0.005**	-0.40	0.057
P20357	**Map2**	1635	Microtubule-associated protein 2	S*GILVPSEK	**-0.65**	**0.005**	-0.66	0.004
Q61165	**Slc9a1**	707	Sodium/hydrogen exchanger 1	IGS*DPLAYEPK	**-0.63**	**0.004**	0.17	0.366
Q8K3X4	**Irf2bpl; Irf2bp2**	13	Probable E3 ubiquitin-protein ligase IRF2BPL; Interferon regulatory factor 2-binding protein 2	RQS*CYLCDLPR	**-0.63**	**0.001**	0.33	0.047
P70698	**Ctps1**	575	CTP synthase 1	SGSSS*PDSEITELK	**-0.61**	**0.009**	0.36	0.089
null	**Srcap**	2771	Snf2-related CREBBP activator protein	TS*ADVEIR	**-0.59**	**0.004**	-0.49	0.011
P81122	**Irs2**	362	Insulin receptor substrate 2	TAS*EGDGGAAGGAGTAGGR	**-0.58**	**0.004**	0.19	0.249
Q02248	**Ctnnb1**	551	Catenin beta-1	RT*SM^GGTQQQFVEGVR	**-0.57**	**0.008**	-0.06	0.754
F7BJB9	**Morc3**	563	MORC family CW-type zinc finger protein 3	RLS*NPPVENSSYK	**-0.57**	**0.002**	-0.29	0.062
Q811L6	**Mast4; Mast1; Mast2**	1436	Microtubule-associated serine/threonine-protein kinase 4; Microtubule-associated serine/threonine-protein kinase 2	SAEPPRS*PLLK	**-0.56**	**0.001**	-0.41	0.007
Q8BG05	**Hnrnpa3**	361	Heterogeneous nuclear ribonucleoprotein A3	SSGSPY*GGGYGSGGGSGGYGSR	**-0.54**	**0.003**	-0.23	0.143
P35569	**Irs1**	3	Insulin receptor substrate 1	#AS*PPDTDGFSDVR	**-0.54**	**2.04E-04**	-0.09	0.418
P97310	**Mcm2**	21	DNA replication licensing factor MCM2	RIS*DPLTSSPGR	**-0.51**	**0.001**	-0.11	0.378
Q9QXZ0	**Macf1**	3889	Microtubule-actin cross-linking factor 1	QGS*FSEDVISHK	**-0.51**	**0.008**	0.23	0.177
Q8K310	**Matr3**	188	Matrin-3	RDS*FDDR	**-0.50**	**0.003**	0.11	0.423
Q9DBR1	**Xrn2**	473	5'-3' exoribonuclease 2	NSSPS*ISPNTSFASDGSPSPLGGIK	**0.50**	**0.003**	-0.41	0.010
E1U8D0	**Soga1**	1300	Protein SOGA1	APS*PTTAAGEESCK	**0.52**	**0.006**	0.11	0.494
Q8BTI8	**Srrm2**	1338	Serine/arginine repetitive matrix protein 2	S*SSELSPEVVEK	**0.53**	**0.006**	0.10	0.561
Q8BIA4	**Fbxw8**	86	F-box/WD repeat-containing protein 8	SRS*PPDRDATEPEPLVDQLIR	**0.57**	**0.003**	-0.24	0.126
Q99K30	**Eps8l2**	217	Epidermal growth factor receptor kinase substrate 8-like protein 2	QPGDS*PQAK	**0.57**	**0.007**	-0.02	0.893

P63058	**Thra**	12	Thyroid hormone receptor alpha	VECGS*DPEENSAR	**0.61**	**0.006**	-0.24	0.208
Q9CQT2	**Rbm7**	108	RNA-binding protein 7	SGSSHASQDASVSYPQHHVGNLS*PTSTSPNSYER	**0.63**	**0.008**	-0.10	0.608
Q9WTQ5	**Akap12**	584	A-kinase anchor protein 12	GPSEAPQEAEAEEGATS*DGEKKR	**0.64**	**0.008**	-0.02	0.908
Q9QXM1	**Jmy**	704	Junction-mediating and -regulatory protein	STAS*PVPCEEQCHSLPTVLQGQEK	**0.67**	**0.005**	-0.29	0.166
P39053	**Dnm1**	774; 777	Dynamin-1	RS*PTS*SPTPQR	**0.67**	**0.002**	-0.31	0.105
Q9Z1T6	**Pikfyve**	1753	1-phosphatidylinositol 3-phosphate 5-kinase	GTAGKS*PDLSSQK	**0.68**	**5.23E-05**	-0.25	0.039
Q8BTI8	**Srrm2**	1343	Serine/arginine repetitive matrix protein 2	SSSELS*PEVVEK	**0.68**	**0.002**	0.13	0.472
Q8C078	**Camkk2**	91	Calcium/calmodulin-dependent protein kinase kinase 2	DQPPEADGQELPLEASDPESRS*PLSGR	**0.75**	**9.91E-05**	-0.14	0.317
P58802	**Tbc1d10a**	407	TBC1 domain family member 10A	AILDAEPGPRPALQPS*PSIR	**0.78**	**2.06E-04**	-0.34	0.039
P43274	**Hist1h1c; Hist1h1t; Hist1h1e; Hist1h1b; Hist1h1d**	102	Histone H1.2; Histone H1.4; Histone H1.5; Histone H1.3	GTGAS*GSFK	**0.79**	**0.006**	0.10	0.663
Q9ESE1	**Lrba**	979	Lipopolysaccharide-responsive and beige-like anchor protein	DS*PISPHFTR	**0.80**	**0.003**	-0.10	0.659
Q6PDN3	**Mylk**	355	Myosin light chain kinase, smooth muscle	VPAIGSFS*PGEDRK	**0.81**	**0.001**	-0.21	0.261
P56402	**Aqp2**	256; 261	Aquaporin-2	QS*VELHS*PQSLPR	**1.02**	**4.83E-04**	0.44	0.064
P40645	**Sox6**	454	Transcription factor SOX-6	TS*PVNLPNK	**1.19**	**0.007**	-0.10	0.783
P40645	**Sox6**	439	Transcription factor SOX-6	S*PTSPTQNLFPASK	**1.40**	**0.002**	0.13	0.708

†Multiple gene symbols are given when a peptide matches sequences in multiple proteins.

Table 4. Phosphopeptides changed most convincingly in PKA-Cβ null cells versus PKA-Cβ intact (P_{mod} < 0.01 and |log(ratio)| > 0.5). PKA-Cα-null data for the same peptides is also given for comparison.

UniProt ID	Gene Symbol	Amino acid number	Annotation	Sequence	Log2 (PKA-Cα null/ PKA-Cα intact)	P_{mod}	Log2 (PKA-Cβ null/ PKA-Cβ intact)	P_{mod}
Q6NZF1	**Zc3h11a**	740	Zinc finger CCCH domain-containing protein 11A	RLS*SASTGKPPLSVEDDFEK	-0.71	0.006	**-1.00**	**0.001**
Q67FY2	**Bcl9l**	118	B-cell CLL/lymphoma 9-like protein	SVS*VDSGEQR	-0.75	0.002	**-0.86**	**0.001**
Q03173	**Enah**	719	Protein enabled homolog	APST*STPEPTR	0.00	0.988	**-0.79**	**0.002**
Q9QZQ1	**Mllt4**	1201	Afadin	ITSVS*TGNLCTEEQSPPPRPEAYPIPTQTYTR	-0.05	0.793	**-0.77**	**0.002**
O08796	**Eef2k**	66	Eukaryotic elongation factor 2 kinase	T*ECGSTGSPASSFHFK	-0.13	0.552	**-0.75**	**0.004**
Q03173	**Enah**	720	Protein enabled homolog	APSTS*TPEPTR	-0.11	0.633	**-0.75**	**0.005**
O55003	**Bnip3**	60	BCL2/adenovirus E1B 19 kDa protein-interacting protein 3	SSHCDS*PPR	0.27	0.222	**-0.70**	**0.007**
Q2VPU4	**Mlxip**	9	MLX-interacting protein	#AADVFM^CS*PR	-0.03	0.897	**-0.68**	**0.010**
Q8BUH8	**Senp7**	12	Sentrin-specific protease 7	RAS*SEIVTEGK	-0.67	8.08E-05	**-0.67**	**8.49E-05**
P20357	**Map2**	1635	Microtubule-associated protein 2	S*GILVPSEK	-0.65	0.005	**-0.66**	**0.004**
Q8VDZ4	**Zdhhc5**	409	Palmitoyltransferase ZDHHC5	SEPSLEPESFRS*PTFGK	-0.27	0.144	**-0.64**	**0.003**
Q8CGF1	**Arhgap29**	1241	Rho GTPase-activating protein 29	ESSEEPALPEGT*PTCQRPR	-0.04	0.743	**-0.63**	**0.001**
Q8VI36	**Pxn**	258	Paxillin	IS*ASSATR	-0.01	0.966	**-0.62**	**0.004**
Q8C6B2	**Rtkn**	518	Rhotekin	T*FSLDAAPADHSLGPSR	-0.01	0.962	**-0.60**	**0.005**
Q8C6B2	**Rtkn**	520	Rhotekin	TFS*LDAAPADHSLGPSR	-0.13	0.423	**-0.60**	**0.002**
A1A535	**Veph1**	422	Ventricular zone-expressed PH domain-containing protein 1	INAESNT*PGSGR	-0.34	0.070	**-0.59**	**0.005**
Q9Z2H5	**Epb41l1**	540	Band 4.1-like protein 1	RLPS*SPASPSPK	-0.17	0.332	**-0.57**	**0.006**
P28661	**Sept4**	68	Septin-4	PQS*PDLCDDDVEFR	-0.02	0.917	**-0.55**	**0.003**
Q8C5R2	**Proser2**	223	Proline and serine-rich protein 2	LAGNEALSPTS*PSK	-0.26	0.119	**-0.55**	**0.004**
Q99MR1	**Gigyf1**	227	GRB10-interacting GYF protein 1	ST*SPDGGPR	-0.05	0.640	**-0.51**	**0.001**
Q99MR1	**Gigyf1**	226	GRB10-interacting GYF protein 1	S*TSPDGGPR	0.05	0.723	**-0.50**	**0.003**
Q60864	**Stip1**	481	Stress-induced-phosphoprotein 1	HDS*PEDVK	-0.12	0.498	**0.57**	**0.005**

Table 5. *Gene Ontology Cellular Component* terms enriched in list of phosphoproteins with altered phosphorylation in PKA-Cα-null cells.

Term	Number	Fold Enrichment	Fisher Exact	Proteins
membrane raft	8	4.3	3.20E-04	EGFR, EFHD2, PRKAR2B, PRKAR1A, PIKFYVE, CXADR, CTNNB1, HDAC6
perinuclear region of cytoplasm	12	2.3	3.90E-03	EGFR, PACS1, EPN3, PRKAR2B, FBXW8, PAK2, SCYL2, PIKFYVE, SPTBN2, RAB3IP, CTNNB1, HDAC6
membrane part	26	1.6	6.40E-03	GPRC5C, ACSS2, CXADR, CHCHD6, CTNNB1, EFHD2, PRKAR2B, PIKFYVE, PRKAA1, SYNPO, SREBF1, EGFR, EPN3, OLFR120, KANSL1, SLC33A1, STIM2, CRB3, EMC4, BNIP3L, PRKAR1A, SPTBN2, GRAMD1C, DNM1, HDAC6, SUCO
cytoplasmic vesicle	11	2	1.90E-02	EGFR, PACS1, SREBF1, ARHGAP21, EPN3, SCYL2, RAN, PIKFYVE, SPTBN2, CXADR, DNM1
integral component of membrane	16	1.6	3.60E-02	SREBF1, EGFR, OLFR120, GPRC5C, KANSL1, SLC33A1, STIM2, CRB3, ACSS2, CXADR, CHCHD6, EMC4, BNIP3L, PIKFYVE, GRAMD1C, SUCO
membrane-bounded vesicle	21	1.4	5.00E-02	SREBF1, PACS1, EGFR, SRP14, EPN3, GPRC5C, RAN, CRB3, CXADR, HNRNPA1, CTNNB1, ARHGAP21, FAM65A, PRKAR2B, RPL30, SCYL2, PIKFYVE, SPTBN2, TUBA1B, DNM1, MDH1

Table 6. *Gene Ontology Cellular Component* terms enriched in list of phosphoproteins with altered phosphorylation in PKA-Cβ-null cells.

Term	Number	Fold Enrichment	Fisher Exact	Proteins
cytoskeleton	23	1.7	2.70E-03	DPF2, SEPT4, ENAH, DYNC1LI2, PDLIM5, AKAP12, IGF2BP2, NEXN, MYO9A, PXN, SMC3, TNKS1BP1, EPB41L1, MACF1, MAP2, MAP4, RANBP2, CDC42EP4, CEP170B, UBXN6, AFAP1, SYNPO, SEPT9
adherens junction	16	1.9	5.10E-03	EGFR, ENAH, PDLIM5, AKAP12, NEXN, CXADR, PXN, TNKS1BP1, EPB41L1, LIMD1, EEF1D, ERC1, EPS8L2, AFAP1, TJP2, SEPT9
cell junction	19	1.7	1.30E-02	CLDN8, EGFR, ENAH, PDLIM5, AKAP12, CXADR, NEXN, PXN, TNKS1BP1, EPB41L1, LIMD1, EEF1D, ERC1, CDC42EP4, EPS8L2, AFAP1, TJP2, SYNPO, SEPT9
plasma membrane	21	1.5	1.90E-02	CLDN8, EGFR, ENAH, IRS2, ZDHHC5, PDLIM5, LRBA, AKAP12, WWC1, ZBTB16, CXADR, PXN, AQP2, TNKS1BP1, EPB41L1, MACF1, MAP4, CDC42EP4, EPS8L2, TJP2, SYNPO
actin cytoskeleton	9	2.1	2.60E-02	ENAH, MACF1, PDLIM5, CDC42EP4, MYO9A, AFAP1, PXN, SEPT9, SYNPO

Table 7. Protein kinases with altered phosphorylation in response to deletion of PKA-Cα or PKA-Cβ

Gene Symbol	Annotation	Amino acid number	Centralized Sequence‡	Log2 (PKA-Cα null/ PKA-Cα intact)	P_{mod}	Log2 (PKA-Cβ null/ PKA-Cβ intact)	P_{mod}	Kinase Class	Effect of phosphorylation on activity†
Camkk2	Calcium/calmodulin-dependent protein kinase kinase 2	85	QELPLEAS*DPESRSP	**0.41**	**0.005**	-0.17	0.169	Other	increases
Camkk2	Calcium/calmodulin-dependent protein kinase kinase 2	91	ASDPESRS*PLSGRKM	**0.75**	**9.91E-05**	-0.14	0.317	Other	n.i.
Cdk18	Cyclin-dependent kinase 18	75	EDLNKRLS*LPMDIRL	**-0.66**	**0.005**	-0.40	0.057	CMGC	n.i.
Cdk18	Cyclin-dependent kinase 18	75	EDLNKRLS*LPMDIRL	**-0.61**	**0.012**	-0.39	0.086	CMGC	n.i.
Cdk18	Cyclin-dependent kinase 18	75	EDLNKRLS*LPMDIRL	-0.24	0.150	**-0.42**	**0.021**	CMGC	n.i.
Cdk18	Cyclin-dependent kinase 18	109	TRMSRRAS*LSDIGFG	**-0.65**	**0.042**	-0.18	0.543	CMGC	n.i.
Eef2k	Eukaryotic elongation factor 2 kinase	66	YYSNLTKT*ECGSTGS	-0.13	0.552	**-0.75**	**0.004**	Atypical	n.i.
Egfr	Epidermal growth factor receptor	695	RELVEPLT*PSGEAPN	**-0.55**	**0.024**	**-0.63**	**0.012**	Tyr	altered receptor internalization
Map4k5	Mitogen-activated protein kinase kinase kinase kinase 5	335	SRAERTAS*EINFDKL	**-0.70**	**0.028**	-0.48	0.112	STE	n.i.
Map4k5	Mitogen-activated protein kinase kinase kinase kinase 5	400	PPKPRVNT*YPEDSLP	**-0.80**	**0.027**	-0.04	0.894	STE	n.i.
Mast4	Microtubule-associated serine/threonine-protein kinase 4	1382	SPLARTPS*PTPQPTS	0.04	0.885	**-0.55**	**0.047**	AGC	n.i.
Mast4 or Mast1 or Mast2	Microtubule-associated serine/threonine-protein kinase 4; Microtubule-associated serine/threonine-protein kinase 2	1436	KSAEPPRS*PLLKRVQ	**-0.559**	0.001	-0.411	0.007	AGC	n.i.
Mylk	Myosin light chain kinase, smooth muscle	355	VPAIGSFS*PGEDRK	**0.81**	**0.001**	-0.21	0.261	CAMK	increases
Nrbp2	Nuclear receptor-binding protein 2	20	ERERERDES*EDESDIL	-0.02	0.870	**-0.42**	**0.002**	Other	n.i.
Pak2	Serine/threonine-protein kinase PAK 2	141	TVKQKYLS*FTPPEKD	**-2.00**	**0.043**	-1.30	0.167	STE	increases
Pak2	Serine/threonine-protein kinase PAK 2	197	TKSIYTRS*VIDPIPA	**-1.30**	**0.039**	-0.21	0.719	STE	increases?
Prkaa1	5'-AMP-activated protein kinase catalytic subunit alpha-1	496	ATPQRSGS*ISNYRSC	**-0.41**	**0.009**	-0.13	0.347	CAMK	decreases
Scyl2	SCY1-like protein 2	677	QGKQKRGS*LTLEEKQ	**-0.47**	**0.006**	0.09	0.541	Other	n.i.
Sik2	Serine/threonine-protein kinase SIK2	342	ERLKSHRS*SFPVEQR	**-0.42**	**0.013**	-0.14	0.333	CAMK	increases?
Slk	STE20-like serine/threonine-protein kinase	777	SKAKDSGS*VSLQETR	-0.21	0.293	**-0.43**	**0.041**	STE	n.i.
Wnk1	Serine/threonine-protein kinase WNK1	165	TSKDRPVS*QPSLVGS	0.09	0.578	**0.42**	**0.020**	Other	n.i.

†Based on information at *PhospoSitePlus* (https://www.phosphosite.org), n.i., no information available. ‡ Asterisks indicate phosphorylated amino acids. R or K in positions -3 and -2 are underlined.

Table 8. AKAPs and cAMP-associated proteins with altered phosphorylation in either PKA-Cα or PKA-Cβ-null cells

UniProt ID	Gene Symbol	Annotation	Amino acid number	Centralized Sequence†	Log_2(PKA-Cα null/ PKA-Cα intact)	P_{mod}	Log_2(PKA-Cβ null/ PKA-Cβ intact)	P_{mod}
O08715	**Akap1**	A-kinase anchor protein 1, mitochondrial	101	TRQVRRRS*ESSGNLP	**-0.41**	0.003	0.00	0.966
Q9WTQ5	**Akap12**	A-kinase anchor protein 12	22	PAESDTPS*ELELSGH	**0.55**	0.035	-0.09	0.716
Q9WTQ5	**Akap12**	A-kinase anchor protein 12	583	AEAEEGAT*SDGEKKR	**0.43**	0.018	0.11	0.490
Q9WTQ5	**Akap12**	A-kinase anchor protein 12	584	EAEEGATS*DGEKKRE	**0.64**	0.008	-0.02	0.908
Q9WTQ5	**Akap12**	A-kinase anchor protein 12	683	KRARKASS*SDDEGGP	**0.51**	0.011	-0.11	0.514
Q9WTQ5	**Akap12**	A-kinase anchor protein 12	684	RARKASSS*DDEGGPR	**0.52**	0.019	-0.20	0.305
Q9WTQ5	**Akap12**	A-kinase anchor protein 12	1292	SNEEQSIS*PEKREMG	0.40	0.061	**0.49**	0.026
Q3UEI1	**Pde4c**	cAMP-specific 3',5'-cyclic phosphodiesterase 4C	301	ELRRSSHT*SLPTAAI	**-0.43**	0.034	0.26	0.173
P70453	**Pde7a**	High affinity cAMP-specific 3',5'-cyclic phosphodiesterase 7A	58	FETERRGS*HPYIDFR	**-0.44**	0.020	-0.40	0.031
Q5EG47	**Prkaa1**	5'-AMP-activated protein kinase catalytic subunit alpha-1	496	ATPQRSGS*ISNYRSC	**-0.41**	0.009	-0.13	0.347
Q9DBC7	**Prkar1a**	cAMP-dependent protein kinase type I-alpha regulatory subunit	83	DSREDEIS*PPPPNPV	**-0.90**	0.001	-0.11	0.599
Q9DBC7	**Prkar1a**	cAMP-dependent protein kinase type I-alpha regulatory subunit	83	DSREDEIS*PPPPNPV	**-1.05**	1.34E-04	-0.09	0.642
Q9DBC7	**Prkar1a**	cAMP-dependent protein kinase type I-alpha regulatory subunit	83	DSREDEIS*PPPPNPV	**-1.01**	3.99E-04	0.05	0.816
P31324	**Prkar2b**	cAMP-dependent protein kinase type II-beta regulatory subunit	112	NRFTRRAS*VCAEAYN	**-1.38**	0.001	-0.29	0.402

†Asterisks indicate phosphorylated amino acids. R or K in positions -3 and -2 are underlined.

Table 9. Phosphopeptides from transcription factor proteins that underwent changes in abundance with PKA-Cα and/or PKA-Cβ deletion

UniProt ID	Gene Symbol	Annotation	Amino acid number	Centralized sequence†	Log2 (PKA-Cα null/ PKA-Cα intact)	P_{mod}	Log2 (PKA-Cβ null/ PKA-Cβ intact)	P_{mod}	TF family
Q3US59	**Atf7**	Cyclic AMP-dependent transcription factor ATF-7	326	TGGRRRRT*VDEDPDE	**-1.19**	0.039	-0.60	0.266	bZIP
Q61103	**Dpf2**	Zinc finger protein ubi-d4	142	DPRVDDDS*LGEFPVS	-0.44	0.061	**-0.59**	0.017	zf-C2H2
Q8K5C0	**Grhl2**	Grainyhead-like protein 2 homolog	2	_____MS*QESDNNK	**0.42**	0.038	-0.11	0.539	CP2
P15066	**Jund (or Jun)**	Transcription factor jun-D (or jun)	100	LGLLKLAS*PELERLI	**-0.69**	0.002	0.07	0.720	bZIP
Q2VPU4	**Mlxip**	MLX-interacting protein	9	AADVFMCS*PRRPRSR	-0.03	0.897	**-0.68**	0.010	bHLH
P40645	**Sox6**	Transcription factor SOX-6	439	KTAEPVKS*PTSPTQN	**1.40**	0.002	0.13	0.708	HMG
P40645	**Sox6**	Transcription factor SOX-6	454	LFPASKTS*PVNLPNK	**1.19**	0.007	-0.10	0.783	HMG
Q9WTN3	**Srebf1**	Sterol regulatory element-binding protein 1	96	KVTPAPLS*PPPSAPA	**-0.80**	0.024	0.22	0.500	bHLH
Q9JM73	**Srf**	Serum response factor	220	TCLNSPDS*PPRSDPT	**0.41**	0.007	-0.05	0.710	SRF
P63058	**Thra**	Thyroid hormone receptor alpha	12	PSKVECGS*DPEENSA	**0.61**	0.006	-0.24	0.208	TH
P62960	**Ybx1**	Nuclease-sensitive element-binding protein 1	174	EKNEGSES*APEGQAQ	**-0.47**	0.020	-0.05	0.792	CSD
Q3UQ17	**Zbtb16**	MCG3834	307	EESGEQLS*PPVEAGQ	-0.44	0.236	**-1.04**	0.012	ZBTB
Q8BIQ6	**Zfp947**	MCG23335	283	FTQKSSLS*IHQMYHT	**0.50**	0.044	0.07	0.768	zf-C2H2
O35615	**Zfpm1**	Zinc finger protein ZFPM1	681	RGSEGSQS*PGSSVDD	**0.68**	0.030	-0.06	0.843	zf-C2H2

†Asterisks indicate phosphorylated amino acids. R or K in positions -3 and -2 are underlined.